

# Effect of extreme pH levels on early larval stages of the Pacific abalone (*Haliotis discus hannai* Ino, 1953)

Dian Yuni Pratiwi<sup>1,2</sup>, Irfan Zidni<sup>2</sup>, Mi-Jin Choi<sup>3</sup>, Young Dae Oh<sup>3</sup>, Tae Min Kim<sup>1</sup>, Han Kyu Lim<sup>1,3,4,\*</sup>

<sup>1</sup> Department of Biomedicine, Health & Life Convergence Sciences, BK21 Four, Mokpo National University, Mokpo 58554, Korea

<sup>2</sup> Department of Fisheries, The Faculty of Fisheries and Marine Science, Universitas Padjadjaran, Sumedang Regency 45363, Indonesia

<sup>3</sup> Smart Aqua Farm Convergence Research Institute, Mokpo National University, Mokpo 58554, Korea

<sup>4</sup> Department of Fisheries Biomedical Sciences, Mokpo National University, Mokpo 58554, Korea

## Abstract

Seawater pH, which can be altered by human activity-induced pollution, potentially affects developmental processes at the early larval stages of Pacific abalone (*Haliotis discus hannai*). This study aimed to examine the effects of extreme seawater pH on these stages in Pacific abalone. Abalone eggs and larvae were exposed to five pH levels (pHs 6, 7, 8, 9, and 10), and several parameters were measured: hatching rate, malformation rate, larval length, DNA damage, oxygen consumption rate, settlement rate, and expression levels of two biomineralization genes (calmodulin and carbonic anhydrase) and one heat stress gene (heat shock protein 90, HSP90). Hatching rates decreased under low (pH 6) and high (pH 9 and 10) pH levels, compared to the control (pH 8). Extremely low and high pHs significantly affected larval length, malformation rate, and DNA damage ( $p < 0.05$ ). At 20 hours post-fertilization (hpf), the oxygen consumption rate was significantly decreased only at pH 6 ( $p < 0.05$ ). However, at 30 hpf, a significant reduction in the oxygen consumption rate was observed only at pHs 9 and 10 ( $p < 0.05$ ). The settlement rate decreased significantly only at pH 10 ( $p < 0.05$ ). Seawater pH affected carbonic anhydrase gene expression in larvae at 30 hpf, but not at 20 hpf, while calmodulin and HSP90 gene expression remained unchanged. In conclusion, extremely acidic and alkaline seawater pHs severely disrupt early larval development in Pacific abalone.

**Keywords:** Pacific abalone, pH levels, Early larval development, Settlement rate

## Introduction

Seawater pH is a critical environmental stressor for marine species resulting in both direct and indirect adverse effects (Wessel

et al., 2018). It significantly affects early developmental stages, critical physiological functions, and skeletal growth (Wessel et al., 2018). The current average pH of the open ocean is 8.1, a decrease of 0.1 units from 8.2 since the Industrial Revolution

Received: Oct 24, 2024 Revised: Dec 20, 2024 Accepted: Feb 10, 2025

\*Corresponding author: Han Kyu Lim

Department of Biomedicine, Health & Life Convergence Sciences, BK21 Four, Mokpo National University, Mokpo 58554, Korea

Tel: +82-61-450-2395, Fax: +82-61-452-8875, E-mail: [limhk@mnu.ac.kr](mailto:limhk@mnu.ac.kr)

This is an Open Access article distributed under the terms of the Creative Commons Attribution Non-Commercial License (<http://creativecommons.org/licenses/by-nc/4.0/>) which permits unrestricted non-commercial use, distribution, and reproduction in any medium, provided the original work is properly cited.

Copyright © 2025 The Korean Society of Fisheries and Aquatic Science

(Liu et al., 2012). This decline in seawater pH is attributable to an increase in CO<sub>2</sub> absorption by the oceans (Caldeira & Wickett, 2003), with pH predicted to drop further by an additional 0.3–0.4 units in accordance with the IS92a scenario by 2100 (Orr et al., 2005) and by 0.77 units by 2300 (Caldeira & Wickett, 2003). Atmospheric CO<sub>2</sub> concentrations are expected to reach 788 parts per million by volume (PPMV) by 2100 (Orr et al., 2005) and 1,900 PPMV by 2300 (Caldeira & Wickett, 2003). In coastal areas, human activities and seasonal variation can cause short-term or temporal fluctuations in pH levels that frequently exceed pH trends observed across decades (Ono et al., 2024). For example, industries producing titanium dioxide via sulfuric acid can produce waste water with a pH of 1–2 (Li et al., 2023). Several industries and domestic activities use NaOH, which can enter the water and increase the pH level (Ghazy et al., 2011). In extreme cases, coastal pH levels might exceed 9 or fall below 7 (Hinga, 2002).

Most aquatic organisms can survive within a pH range of 6.0 and 9.0, while macroinvertebrates can tolerate pH levels between 6.5–8.5. However, some marine organisms can survive in water outside this pH range. Sensitivity to pH changes varies significantly among marine ecosystems (Ghazy et al., 2011), life stages, and species (van Colen et al., 2012). Several studies have shown that mollusks are susceptible to pH-related stress, especially in their early life stages. Wessel et al. (2018) reported that a low pH of 7.6–7.7 caused European abalone (*Haliotis tuberculata*) larvae to be smaller than the controls. The number of malformed or unshelled larvae was also increased at low pHs. The hatching rate and normal larval growth of donkey's ear abalone (*Haliotis asinina*) were significantly reduced at pH 7.4 and 7.6, compared to the controls (Tahil & Dy, 2016).

Abalone, widely distributed across tropical and temperate coastal areas, is an economically important molluscan species. The global value of abalone exports increased from USD 36.79 million in 1976 to USD 644.16 million in 2020 (FAO, 2022). In Korea, the production of farmed abalone increased significantly from 20 tons in 2000 to 22,078 tons in 2022 (KOSIS, 2022). Pacific abalone (*Haliotis discus hannai*) accounts for the highest production volume in South Korea (KOSIS, 2022). The effect of decreasing pH due to elevated pCO<sub>2</sub> on Pacific abalone larvae was studied by Kimura et al. (2011) and Li et al. (2013), with reductions in pH ranging between 7.41–8.02 and 7.30–8.20, respectively. However, research examining the effects of decreasing or increasing pHs across a broader range remains limited. Research on the impact of extreme pH conditions will

provide fundamental data that is crucial to understand the sensitivity of abalone larvae to environmental pH fluctuations.

Hatching rate, larval length, malformation rate, oxygen consumption rate, and settlement rate are commonly studied parameters used to evaluate the effects of pH on larval abalone. In addition to these parameters, DNA damage has been analyzed using comet assays to investigate the effects of environmental stress on several aquatic organisms, including Mediterranean mussel (*Mytilus galloprovincialis*) (Braga et al., 2020), backwater hard clam (*Meretrix casta*) (Praveen Kumar et al., 2014), and yellow clam (*Paphia malabarica*) (Praveen Kumar et al., 2014). However, the use of comet assays to analyze the effects of pH on abalone larvae remains unexplored. Acidification has been observed to disrupt calcification and shell formation in mollusks (Wessel et al., 2018). Therefore, it is critical to investigate the expression of genes involved in calcification, such as calmodulin and carbonic anhydrase (Sharker et al., 2021). Calmodulin, an intracellular calcium-signaling mediator, is crucial for controlling calcium absorption and transport during biomineralization and can also serve as a stress indicator (Liu et al., 2012). Carbonic anhydrase catalyzes the change of CO<sub>2</sub> to bicarbonate ions and protons (Sharker et al., 2021). In addition, the expression of heat shock proteins (HSPs) has been widely analyzed to determine an organism's stress response. HSP expression is induced by heat stress and various environmental stimuli (Lee, 2023), including pH (Qian et al., 2012).

This study aimed to investigate the effects of extreme seawater pH on the early larval stages of Pacific abalone. The parameters analyzed included the hatching rate, larval length, malformation rate, DNA damage, oxygen consumption rate, settlement rate, expression levels of biomineralization genes (calmodulin and carbonic anhydrase), and stress-related genes (HSP90). Larvae were examined at 20 and 30 hours post fertilization (hpf), corresponding to the free-swimming trochophore and veliger stages, respectively. Additionally, the settlement rate was assessed at 96 hpf, during the premetamorphic stage.

## Materials and Methods

### Fertilized egg collection and larvae rearing

Fertilized Pacific abalone eggs were collected from a commercial abalone hatchery (Haenam, Jeollanam Province, Korea). The eggs were placed in plastic bags under oxygen pressure and returned to the Laboratory of Marine and Fisheries Resources at Mokpo National University. The fertilized eggs were main-

tained at 18°C and 32 practical salinity units (PSU) without aeration, replicating the hatchery seawater conditions. Embryonic development was monitored utilizing a stereomicroscope (Leica MZ10F, Leica Microsystems, Heerbrugg, Germany) at a 6.3 × 100 µm magnification. The experiment used embryos at four hpf during which most embryos had reached the morula stage.

### Experimental design

To investigate the effects of extreme pH on early larval development, embryos at the morula stage were divided into five pH conditions (6, 7, 8, 9, and 10), using three replicate tanks for each pH treatment. We selected pH levels 6–9 based on the pH tolerance of most aquatic organisms, while pH 10 was chosen to assess sensitivity beyond tolerance limits. Local seawater pH typically ranges between 7.96–8.15. For the experimental design with 1-unit pH differences, pH 8 was chosen as the control. Embryos were incubated in 1 L of filtered seawater at 21°C and 32 PSU until 30 hpf. Since abalone larvae are lecithotrophic, deriving food from egg yolks, no feed was provided during the experiment. Seawater pH was measured using a YSI water quality analyzer (YSI Professional Plus; YSI, Yellow Springs, OH, USA), calibrated using three-point calibration buffers with pHs 4, 7, and 10. This water analyzer measured the pH using the NBS scale. The pH was modified using 1 M hydrochloric acid (HCl) and 1 M NaOH solution.

### Hatching rate, larval length, malformation rate

The hatching rate was monitored using a stereomicroscope (Leica MZ10F, Leica Microsystems) by randomly sampling three 1 mL replicates per tank ( $n = 9$  per pH treatment). The hatching rate was measured by calculating the number of hatched larvae compared to the number of fertilized eggs and multiplied by 100. Larvae at 20 and 30 hpf were sampled and fixed in 70% ethanol to measure the larval length and malformation rate. The malformation rate was measured by subsampling three 1 mL replicates per tank ( $n = 9$  per pH treatment) using a stereomicroscope (Leica MZ10F, Leica Microsystems). The assessment of the malformation rate of 20 hpf larvae was based on abnormalities in the prototrochal ciliary band, apical tuft, and shell (Tahil & Dy, 2016), while at 30 hpf it was based on abnormal bodies, abnormal shells, or unshelled larvae (Li et al., 2013). Larval lengths at 20 and 30 hpf were measured using a stereomicroscope (Leica MZ10F, Leica Microsystems) at a magnification of 6.3 × 100 µm.

### DNA damage

DNA damage was evaluated using alkaline single-cell electrophoresis (CometAssay, Trevigen, Gaithersburg, MD, USA). After pH treatment, larvae of 20 and 30 hpf were sampled and homogenized in a buffer containing 1X HBSS, 10% dimethyl sulfoxide, and 20 mM EDTA with a pH of 7.0–7.5. Samples were centrifuged at 845×g for 5 min at 4°C. The cell pellet was then diluted in chilled phosphate-buffered saline and combined with molten LMAgarose at a ratio of 1:10 (v/v). A 100 µL aliquot was immediately pipetted onto the CometSlide™ and incubated at 4°C in the dark for 10 min. Then, slides were submerged in a lysis solution at 4°C in the dark for 30 min before being placed in an alkaline solution (NaOH 8 g and 5 mL 200 mM EDTA L<sup>-1</sup> distilled water) for another 30 min. Electrophoresis was carried out using an alkaline electrophoresis solution (NaOH 8 g and 2 mL 500 mM EDTA L<sup>-1</sup> distilled water) at 21 V for 30 min. Slides were then immersed twice in distilled water for 10 min each, followed by a 5-minute immersion in 70% ethanol. Samples were stained with SYBR Gold for 30 min and observed using a fluorescence microscope (DM 2500, Leica, Wetzlar, Germany) for analysis. Fifty cells per treatment were scored randomly and analyzed using the Comet Assay IV Lite System (Instem, Staffordshire, UK). Tail intensity (% tail DNA) was used to express cellular DNA damage.

### Oxygen consumption rate

After pH treatment, 10 mL samples of 20 and 30 hpf larvae were subsampled and placed in glass bottles with an oxygen sensor spot (SP-PSt3-NAU, PreSens, Regensburg, Germany) affixed to the inner wall. Screw caps and parafilm were used to tightly and carefully seal the glass bottles. The initial oxygen concentration was immediately recorded utilizing a fiber optic oxygen meter, the Fibox 4 (PreSens), connected to a polymer optical cable (POF, PreSens). Reactive oxygen spots were calibrated by scanning the integrated barcode reader sensor of the oxygen meter, according to the manufacturer's instructions. After one hour, the oxygen sensor in each bottle was scanned again to record the final oxygen level. Larvae in each bottle were then counted, and oxygen consumption was estimated by deducting the final oxygen concentration from the initial value and dividing by the number of larvae. The data are expressed as nmol.larvae<sup>-1</sup>.h<sup>-1</sup>.

### Settlement rate

The larval settlement rate was assessed using premetamorphic 96-hour post-fertilization (hpf) veliger larvae, which were com-

petent to settle based on the presence of a third tubule on the cephalic tentacle (Mzozo et al., 2023). Fifteen 10-liter plastic aquaria were filled with 8 L of seawater at different pH levels, with 3 replicate tanks per treatment. Two vertical polycarbonate plates (10 cm × 15 cm), covered with diatoms, which served as live food sources and factors to encourage natural settlement, were inserted in each tank. After estimating the larval density, 5 mL of larvae were distributed into each tank. The settlement rate was measured after 24 hours by calculating the number of larvae that settled on the two plates and dividing by the total number of initially incubated larvae.

### Biom mineralization and stress-related gene expression

#### RNA extraction and cDNA synthesis

Abalone larvae at 20 and 30 hpf were sampled and immediately frozen in liquid nitrogen. Before RNA extraction, the samples were frozen at  $-80^{\circ}\text{C}$ . Total RNA was isolated using RiboEx (GeneAll Biotechnology, Seoul, Korea) according to the manufacturer's instructions. RNA purity was determined using a NanoDrop™ One<sup>C</sup> (Thermo Fisher Scientific, Wilmington, MA, USA) instrument. Subsequently, high-quality total RNA was reverse transcribed into cDNA using the Maxima First-Strand cDNA Synthesis kit (K1641, Thermo Fisher Scientific), following the manufacturer's instructions. A polymerase chain reaction was performed under the following conditions: initial denaturation at  $25^{\circ}\text{C}$  for 10 min, annealing at  $65^{\circ}\text{C}$  for 30 min, and a final extension at  $85^{\circ}\text{C}$  for 5 min. The synthesized cDNA was stored at  $-80^{\circ}\text{C}$  until further analysis.

#### Gene expression levels

Two biomineralization genes (calmodulin and carbonic anhydrase) and one heat stress-related gene (HSP90) were analyzed in this study. Specific primers used are listed in Table 1. Gene

amplification was performed using a reaction mix comprising 2  $\mu\text{L}$  of cDNA, 10  $\mu\text{L}$  of 2× qPCR mix buffer, 0.6  $\mu\text{L}$  (10 mM) each of forward and reverse primers, and 6.8  $\mu\text{L}$  of nuclease-free water. Pre-denaturation was performed at  $50^{\circ}\text{C}$  for 2 min, followed by 40 cycles of denaturation at  $95^{\circ}\text{C}$  for 15 s, annealing at  $60^{\circ}\text{C}$  for 30 s, and extension at  $72^{\circ}\text{C}$  for 30 s. Amplification results were verified using PikoReal software 2.1, and the  $2^{-\Delta\Delta\text{Ct}}$  method was used for comparison with previously published Ct values. Ribosomal protein L3 (*RPL3*) was used as a reference gene, as described by Choi et al. (2022).

#### Statistical analysis

The Shapiro-Wilk Test was applied to ensure that all data were normally distributed. Normally distributed data were evaluated with one-way analysis of variance (ANOVA) and Tukey's post hoc test. A *t*-test was also used to compare the two larval stages at each pH. For non-normally distributed data, the Kruskal-Wallis test was used, followed by Dunn's post hoc test. Additionally, a Wilcoxon test was applied to compare changes between the two larval stages at each pH. Two-way ANOVA and Aligned Rank Transform ANOVA were performed to evaluate interaction effects between pH and larval age ( $p < 0.05$ ). We performed Spearman's Rho Correlation to assess the correlation between parameters. All data were analyzed using SPSS version 25.0 (IBM, Armonk, NY, USA).

## Results

#### Hatching rate, larval length, and malformation rate

The highest hatching rate of Pacific abalone was observed in the control group at pH 8 ( $86.40 \pm 2.01\%$ ). The lowest hatching rate was observed at pH 10 ( $11.17 \pm 0.83\%$ ) and significantly differed from those observed with other pH treatments. The

**Table 1. Specific primers for gene expression analysis**

Gene name	Sequence (5'–3')	References
RPL3	F: 5'-AGTCCTTCCCTAAGGATGACAAG-3' R: 5'-GCCTCCACAACCTCCTTCTTATT-3'	Choi et al. (2022)
Carbonic anhydrase	F: 5'-GAGAAACGCTACGATGCTG-3' R: 5'-GCTCTCCTTCACACAATGG-3'	Sharker et al. (2021)
Calmodulin	F: 5'-AGCCTTTTCGACAAAGACGG-3' R: 5'-TCTGGCCATCATTGTCAGGA-3'	Designed for the study
HSP90	F: 5'-TTGACGAGTACTGTGTCCAG-3' R: 5'-ACCAGACGATTGGAAACCAC-3'	Lee et al. (2023)

RPL3, Ribosomal protein L3; HSP, heat shock proteins.

hatching rates were not significantly different between pH 6, 7, and 9, nor between pH 7 and 8 (Fig. 1).

For a larval length of 20 hpf, substantial reductions were noted in the lowest pH (pH 6) and highest pH (pH 10) treatments compared to the control (pH 8;  $317.86 \pm 6.06 \mu\text{m}$ ). The shortest larval length was recorded at pH 10 ( $284.83 \pm 8.49 \mu\text{m}$ ), followed by pH 6 ( $286.56 \pm 10.04 \mu\text{m}$ ). In the case of 30 hpf larvae, the larval length at pH 8 ( $377.14 \pm 7.41 \mu\text{m}$ ) was not significantly different from that at pH 9 ( $346.74 \pm 10.29 \mu\text{m}$ ), but it differed from the other pH levels. The shortest larval length was observed at pH 6 ( $290.78 \pm 9.60 \mu\text{m}$ ), followed by pH 10 ( $315.02 \pm 5.22 \mu\text{m}$ ). Substantial differences in larval length were observed between 20 and 30 hpf at pHs of 8–10 (Fig. 2).

The malformation rates of larvae at 20 and 30 hpf are presented in Fig. 3. The malformation rate of 20 hpf larvae at pH 6, 9, and 10 was increased significantly from the control (pH 8). At 20 hpf, the malformation rates of larvae at pH 6 and 10 were  $46.59 \pm 3.54\%$  and  $43.03 \pm 4.125\%$ , respectively. Normal and abnormal trochophore larvae were observed at pHs 6 and 10, but none showed shell formation (Fig. 4A and 4E). Meanwhile, at pH 9, some larvae showed shell formation (Fig. 4D) despite the relatively high malformation rate ( $39.32 \pm 2.91\%$ ). Almost all larvae at pH 7 and 8 and 20 hpf showed the presence of a shell (Fig. 4B and 4C). The malformation rates at pH 7 and 8 were  $27.27 \pm 2.94\%$  and  $18.28 \pm 1.65\%$ , respectively.

The malformation rates of 30 hpf larvae at pH 6, 9, and 10 were also significantly higher than those of the control (pH 8) (Fig. 3). At pH 6, 9, and 10, the malformation rates were  $88.85$

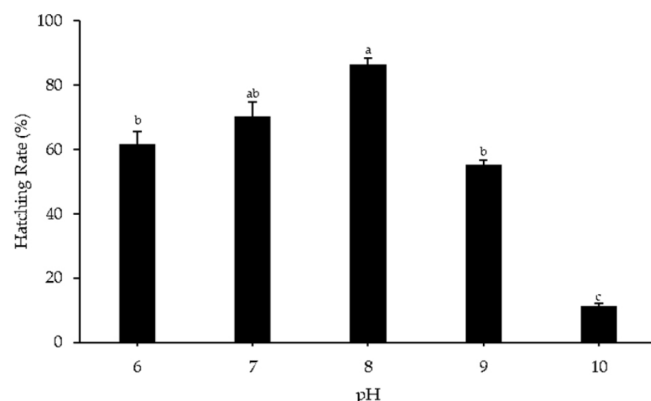


**Fig. 1. The hatching rates of Pacific abalone at various pH conditions are presented, with lowercase letters demonstrating significant differences between the pH treatments ( $p < 0.05$ ).**

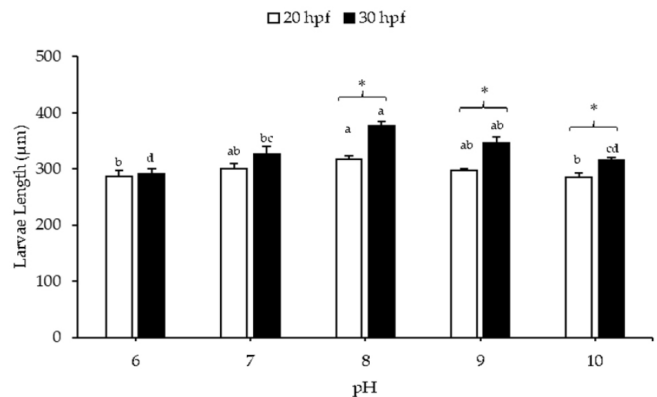


**Fig. 2. Larval lengths of Pacific abalone larvae grown under various pH conditions.** Lowercase letters demonstrate significant differences between pH treatments for each larval stage and asterisks demonstrate significant differences between larval stages ( $p < 0.05$ ).

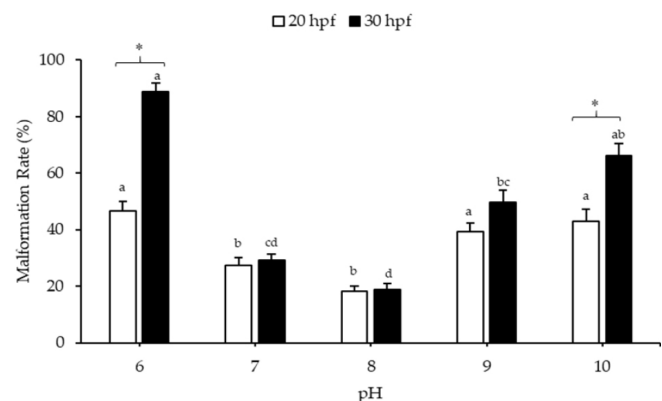


**Fig. 3. Malformation rate of Pacific abalone larvae cultivated under various pH conditions.** Lowercase letters demonstrate significant differences between the pH treatments for each larval stage and asterisks demonstrate significant differences between larval stages ( $p < 0.05$ ).

$\pm 3.06\%$ ,  $49.58 \pm 4.32\%$ , and  $66.24 \pm 4.13\%$ , respectively. Although some larvae could develop into normal veligers at pH 6 and 10, over 50% were aberrant (Fig. 4F and 4J). At pH 8, the larvae at 30 hpf had the lowest malformation rate ( $18.74 \pm 2.22\%$ ). At pH 6 and 10, the malformation rate of larvae at 30 hpf was significantly higher than that of larvae at 20 hpf.

## DNA damage

The recorded DNA damage in Pacific abalone larvae under various pH treatments is shown in Fig. 5. At 20 and 30 hpf, the DNA damage of larvae was significantly higher at pH 6, 9, and



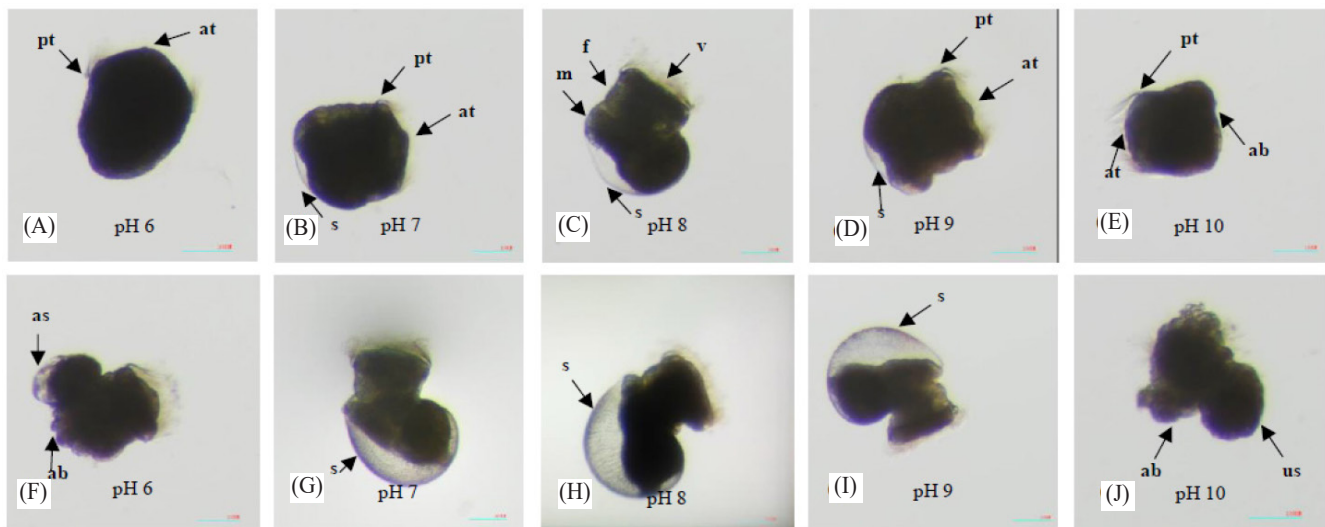


**Fig. 4. The morphology of Pacific abalone larvae grown under various pH conditions.** Top: 20 hpf larvae; Bottom: 30 hpf larvae. (A) normal trochophore larvae; (B and D) normal trochophore larvae with shells; (C) normal early veliger larvae; (E) abnormal trochophore larvae; (F) veliger larvae with abnormal body and shell; (G–I) normal veliger larvae; (J) veliger larvae with abnormal body and no shell. Arrows indicate attributes: prototrochal ciliary band (pt), apical tuft (at), foot (f), mantle (m), shell (s), velum (v), unshelled (us), abnormal shell (as), abnormal (ab).

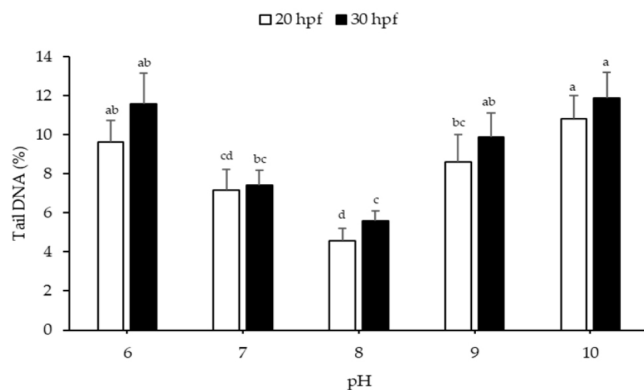


**Fig. 5. DNA damage in Pacific abalone larvae grown under various pH conditions.** Lowercase letters demonstrate significant differences between pH treatments for each larval stage ( $p < 0.05$ ).

10, compared to the control (pH 8). The highest DNA damage was observed at pH 10 for larvae at both 20 and 30 hpf, with values of  $10.83 \pm 1.15\%$  and  $11.85 \pm 1.32\%$ , respectively.

#### Oxygen consumption rate

Our findings regarding the effects of pH on the oxygen consumption rate of Pacific abalone larvae are shown in Fig. 6. At pH 8, the larvae at 20 and 30 hpf had the highest oxygen con-

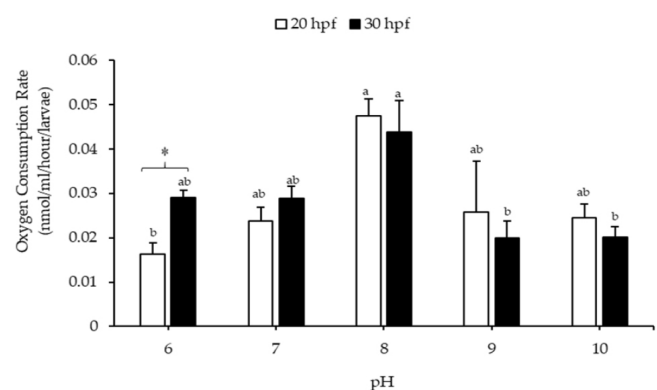


**Fig. 6. Oxygen consumption rate of pacific abalone larvae grown under various pH conditions.** Lowercase letters demonstrate significant differences between pH treatments for each larval stage and asterisks demonstrate significant differences between larval stages ( $p < 0.05$ ).

sumption rates, with values of  $0.0475 \pm 0.0038$  and  $0.0437 \pm 0.0071$   $\text{nmol.larvae}^{-1}.\text{h}^{-1}$ , respectively. The oxygen consumption rate of 20 hpf larvae decreased significantly at pH 6, whereas for 30 hpf larvae, it decreased at pH 9 and 10, compared to the control. Additionally, oxygen consumption rates in 20 and 30 hpf larvae were significantly different at pH 6.

### Settlement rate

Highly significant differences ( $p < 0.05$ ) were observed in the number of attached larvae at pH 10 and the control (pH 8). The lowest settlement rate was recorded at pH 10 ( $1.27 \pm 0.093\%$ ). However, no significant differences were found between pH 6, 7, 9, and the control (Fig. 7).

### Biom mineralization and stress-related gene expression

Fig. 8A depicts the relative mRNA expression levels of the calmodulin gene in Pacific abalone larvae, standardized to *RPL3* expression levels under different pH conditions. Calmodulin expression levels in larvae at 20 and 30 hpf were not significantly affected by pH ( $p > 0.05$ ). The calmodulin expression value at 20 hpf was higher than that at 30 hpf, especially at pH 10. Fig. 8B illustrates carbonic anhydrase expression levels in Pacific abalone under various pH treatments. At 20 and 30 hpf, the expression levels of carbonic anhydrase showed different trends. At 20 hpf, the highest carbonic anhydrase gene expression level was recorded at pH 6 ( $2.72 \pm 0.95$ -fold change); the level decreased as the pH increased, although not significantly. Meanwhile, at 30 hpf, the highest expression was observed at pH 8 ( $1.00 \pm 0.05$ -fold change), and this value was significantly different from that observed with other pH treatments ( $p < 0.05$ ). Additionally, carbonic anhydrase expression was higher at 20 hpf than at 30 hpf, especially at pH 6. HSP90 expression levels at 20 and 30 hpf remained unaffected by pH ( $p > 0.05$ ) (Fig. 8C).

### Interaction effects and correlation test

Table 2 displays the interaction effect between pH and larval age. Only larval length and malformation rate showed significant

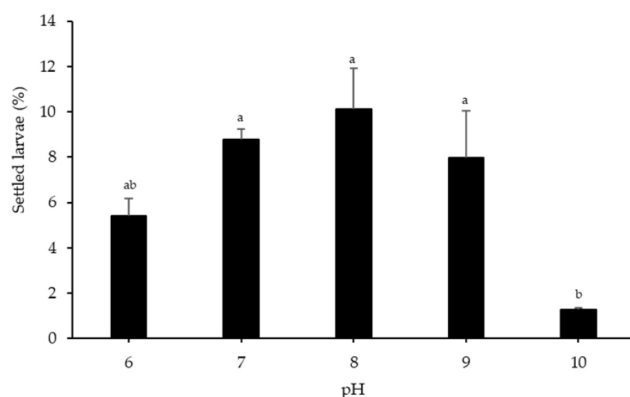


**Fig. 7. Settlement rate of Pacific abalone larvae grown under various pH conditions.** Lowercase letters demonstrate significant differences between pH treatments ( $p < 0.05$ ).

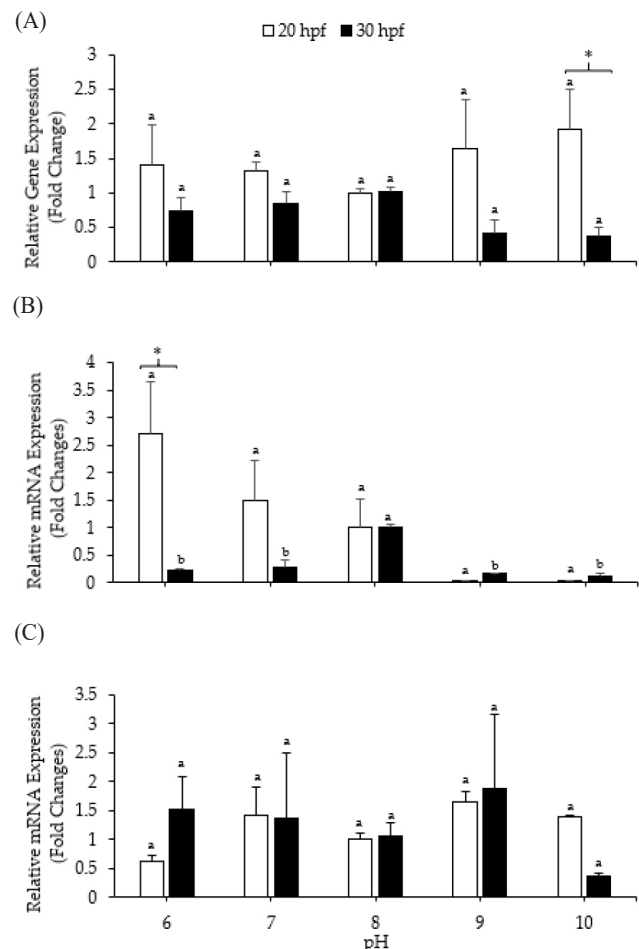


**Fig. 8. Relative mRNA expression levels in Pacific abalone (*Haliotis discus hannai*) larvae (A) calmodulin, (B) carbonic anhydrase I, and (C) HSP90.** Levels were standardized to those of *RPL3* expression under different pH conditions. Lowercase letters demonstrate significant differences between pH treatments for each larval stage and asterisk letters demonstrate significant differences between larval stages ( $p < 0.05$ ). HSP, heat shock proteins; *RPL3*, Ribosomal protein L3.

cant interaction between pH and larval age. Table 3 displays the correlation coefficient matrix of the study parameters. Most of the parameters showed a correlation with more than one other parameter. However, no correlation was found between the oxygen consumption rate and the expression of the HSP90 gene with any other parameters.

## Discussion

The survival and growth of early-life-history-stage abalone are

**Table 2. The interaction effects of pH and larval age for each study parameter**

Parameter	Source	df	F-value	p-value
Larval length	pH	4	15.937	0.000***
	Larval age	1	45.127	0.000***
	pH × Larval length	4	4.628	0.002**
Malformation rate	pH	4	85.119	0.000***
	Larval age	1	76.620	0.000***
	pH × Larval length	4	15.868	0.000***
Dna damage	pH	4	10.775	0.000***
	Larval age	1	2.504	0.114
	pH × Larval length	4	0.146	0.965
Oxygen consumption rate	pH	4	7.946	0.001**
	Larval age	1	0.056	0.816
	pH × Larval length	4	1.243	0.325
HSP90 expression	pH	4	1.014	0.424
	Larval age	1	0.071	0.793
	pH × Larval length	4	1.751	0.178
Calmodulin expression	pH	4	0.082	0.987
	Larval age	1	12.339	0.002**
	pH × Larval length	4	1.769	0.175
Carbonic anhydrase I expression	pH	4	3.426	0.027*
	Larval age	1	6.248	0.027*
	pH × Larval length	4	2.749	0.057

\* $p < 0.05$ , \*\* $p < 0.01$ , \*\*\* $p < 0.001$ .

HSP, heat shock proteins.

critical for determining the size of the adult abalone population (Tahil & Dy, 2016). A decline in the adult population results in a concomitant reduction in output levels and overall economic performance. Previous research has shown that the growth of abalone larvae is affected by the seawater pH (Wessel et al., 2018). Studies assessing the effects of varying seawater pH levels on abalone larvae and other mollusks remain limited. This work represents the first investigation into the effects of extreme seawater pH on the early larval developmental stages of Pacific abalone.

Our findings indicate that extreme pH levels significantly affect the hatching rate of this species. The hatching ability of Pacific abalone eggs remains viable across all pH treatments. However, a significant decrease in the hatching rate was observed upon treatment with a very low pH of 10. This reduction is attributed to the introduction of NaOH into the seawater, which then permeates the egg and hampers embryogenesis. Elevated pH levels can also result in lime deposition on the external surface of the egg, impeding the ingress of essential

nutrients from the external environment, thereby hindering the hatching process (Saad et al., 2023). Huo et al. (2019) observed disparate outcomes in the hatching of Geoduck clam (*Panopea japonica*) eggs, revealing a significant decrease in hatching rate when exposed to acidic water with a pH of 6.8, compared to alkaline water with a pH of 9.2. According to Jiang et al. (2021), acidic water can reduce pH, resulting in the softening and decreased flexibility of the egg membrane, which facilitates membrane rupture and embryo mortality. Previous studies have documented reductions in hatching rates when exposed to lower pH levels, as compared to control conditions in many species, including the donkey's ear abalone (Tahil & Dy, 2016), and Baltic tellin (*Macoma balthica*) (van Colen et al., 2012).

At 20 hpf, differences in larval length were observed only between pH 8 (control), and pHs 6 and 10. Meanwhile, in 30 hpf larvae, differences in length occurred between pH 8 (control) and pH 6, 7, and 10. It is hypothesized that the observed phenomenon can be attributed to the effect of the duration of each pH treatment on larval development. Kapsenberg et al. (2018) reported a positive correlation between the duration of pH treatments and the probability of experiencing delayed larval development. This result is in contrast with research involving European abalone, which showed that a change in pH from 8 to 7.6 significantly affected the development of larvae at 20 and 30 hpf (Wessel et al., 2018). This indicates that sensitivity to pH varies between species (van Colen et al., 2012).

In this study, larval development at extremely low pH (pH 6) was delayed, and malformation rates were higher than at pH 10. This is in accordance with findings on the Geoduck clam, which showed that acidic pH reduces larval length more than alkaline conditions. Alkaline environments are preferable to acidic circumstances for calcification. At alkaline pH values, seawater calcium carbonate is more saturated, which promotes the synthesis and stability of calcium carbonate, thereby accelerating larval growth and shell formation. Meanwhile, low pH conditions delay mineralization, result in shorter larval lengths, and inhibit shell formation (Huo et al., 2019). The malformation rate at control (pH 8) was less than 20% but greater than 10%. The result is similar to the experiment performed by Li et al. (2013), who used the same species and figured out that the malformation rate was less than 20 but greater than 10% at pH 7.9 and 8.2. This is likely due to low-quality egg batches (Nagy et al., 2024) and genetic factors (Lorenzo-Felipe et al., 2021).

In this experiment, treatment at pH 8 resulted in the lowest DNA damage values in larvae at 20 and 30 hpf, significantly dif-



**Table 3. Correlation coefficient matrix of the study parameters**

Spearman's rho correlation	Hatching rate	Larva length	Malformation rate	DNA damage	Oxygen consumption rate	Settlement rate	HSP90 expression	Calmodulin expression	Carbonic anhydrase I expression
<b>20 hpf</b>									
Hatching rate	1.000	.900 <sup>1)</sup>	-0.700	-900 <sup>1)</sup>	0.200	.900 <sup>1)</sup>	-0.300	-1.000 <sup>1)</sup>	0.500
Larva length	.900 <sup>1)</sup>	1.000	-900 <sup>1)</sup>	-1.000 <sup>2)</sup>	0.500	1.000 <sup>2)</sup>	0.100	-900 <sup>1)</sup>	-900 <sup>1)</sup>
Malformation rate	-0.700	-900 <sup>1)</sup>	1.000	.900 <sup>1)</sup>	-0.700	-900 <sup>1)</sup>	-0.300	0.700	0.200
DNA damage	-900 <sup>1)</sup>	-1.000 <sup>1)</sup>	.900 <sup>1)</sup>	1.000	-0.500	-1.000 <sup>2)</sup>	-0.100	.900 <sup>1)</sup>	-0.100
Oxygen consumption rate	0.200	0.500	-0.700	-0.500	1.000	0.500	0.500	-0.200	-0.700
Settlement rate	.900 <sup>1)</sup>	1.000 <sup>2)</sup>	-900 <sup>1)</sup>	-1.000 <sup>2)</sup>	0.500	1.000	0.100	-900 <sup>1)</sup>	0.100
HSP90 expression	-0.300	0.100	-0.300	-0.100	0.300	0.100	1.000	0.300	-0.700
Calmodulin expression	-1.000 <sup>2)</sup>	-900 <sup>1)</sup>	0.700	.900 <sup>1)</sup>	-0.200	-900 <sup>1)</sup>	0.300	1.000	-0.500
Carbonic anhydrase I expression	0.500	0.100	0.200	-0.100	-0.700	0.100	-0.700	-0.500	1.000
<b>30 hpf</b>									
Hatching rate	1.000	0.500	-0.700	-900 <sup>1)</sup>	0.800	.900 <sup>1)</sup>	0.000	1.000 <sup>2)</sup>	1.000 <sup>2)</sup>
Larva length	0.500	1.000	-900 <sup>1)</sup>	-0.800	0.100	0.800	0.000	0.500	0.500
Malformation rate	-0.700	-900 <sup>1)</sup>	1.000	.900 <sup>1)</sup>	-0.300	-900 <sup>1)</sup>	0.200	-0.700	-0.700
DNA damage	-900 <sup>1)</sup>	-0.800	.900 <sup>1)</sup>	1.000	-0.500	-1.000 <sup>2)</sup>	-0.100	-900 <sup>1)</sup>	-900 <sup>1)</sup>
Oxygen consumption rate	0.800	0.100	-0.300	-0.500	1.000	0.500	-0.300	0.800	0.800
Settlement rate	.900 <sup>1)</sup>	0.800	-900 <sup>1)</sup>	-1.000 <sup>2)</sup>	0.500	1.000	0.100	.900 <sup>1)</sup>	.900 <sup>1)</sup>
HSP90 expression	0.000	0.000	0.200	-0.100	-0.300	0.100	1.000	0.000	0.000
Calmodulin expression	1.000 <sup>2)</sup>	0.500	-0.700	-900 <sup>1)</sup>	0.800	.900 <sup>1)</sup>	0.000	1.000	1.000 <sup>2)</sup>
Carbonic anhydrase I expression	1.000 <sup>2)</sup>	0.500	-0.700	-900 <sup>1)</sup>	0.800	.900 <sup>1)</sup>	0.000	1.000 <sup>2)</sup>	1.000

<sup>1)</sup> Correlation is significant at the 0.05 level (2-tailed).

<sup>2)</sup> Correlation is significant at the 0.01 level (2-tailed).  
HSP, heat shock proteins.

fering from those at pH 6, 9, and 10. This outcome is attributed to the induction of reactive oxygen species (ROS) release owing to pH changes (Wu et al., 2016). Similarly, a reduction in pH acts as a stressor that, when combined with osmotic regulation, can modify the body's antioxidant capacity (Kim et al., 2023). Ultimately, an antioxidant capacity lower than ROS generation can result in DNA damage (Wu et al., 2016). DNA damage, resulting in the loss of genetic material, is a significant indicator of how pH affects larvae, as it may cause chromosomal instability and subsequent pathological alterations in cells and tissues (Augustyniak et al., 2014). Increased DNA damage in aquatic organisms under low pHs or alkaline treatments has been reported in Mediterranean mussels (Braga et al., 2020).

The oxygen consumption rate is a key indicator of health in marine organisms, providing insight into stressful environmental conditions (Harris et al., 1999). According to this study, extremely low (pH 6) or high (pH 9 and 10) pHs considerably reduced the oxygen consumption rate of Pacific abalone larvae. Metabolic depression is often a short-term energy storage mechanism for surviving stressful situations. Consequently, larvae can increase their chances of survival during a difficult period by conserving most of their energy for maintenance at the expense of other functions. However, long-term exposure to pH stress can reduce larval survival (Martel et al., 2022). A decrease in metabolic rate can also occur due to decreased enzyme efficiency (Mangan et al., 2017). A significant decrease in oxygen consumption was observed under low and high pH stress in juvenile Greenlip abalone (*Haliotis laevis*), cultivated for 50–68 days when pH levels were altered using HCl and NaOH (Harris et al., 1999). Alternatively, pH stress caused a significant increase in oxygen consumption rate in Eastern oyster (*Crassostrea virginica*) larvae (Schwaner et al., 2023). Meanwhile, Blue mussels (*Mytilus edulis*) exhibited variable oxygen consumption rates between short-term (6 h) and medium-term exposure (2 weeks) (Mangan et al., 2017). Thus, it is hypothesized that metabolic responses to pH stress are influenced by the duration of exposure (Mangan et al., 2017).

This study found that pH did not affect calmodulin gene expression in Pacific abalone larvae at 20 and 30 hpf. This finding is in contrast with the results described by Liu et al. (2012), who observed a significant downregulation of calmodulin gene expression in pearl oysters (*Pinctada fucata*) at pH 7.7. According to Xin et al. (2022), calmodulin is crucial for regulating calcium homeostasis in bivalves and its downregulation may inhibit calcification. Although pH did not have a significant

effect on calmodulin in this study, prolonged pH exposure may eventually disrupt calmodulin expression and interfere with the calcification process.

Carbonic anhydrase plays a crucial role in facilitating biological calcification in several marine invertebrates. Carbonic anhydrase facilitates the reversible hydration of carbon dioxide, producing bicarbonate ions ( $\text{HCO}_3^-$ ) and hydrogen ions ( $\text{H}^+$ ), which are crucial for providing the dissolved inorganic carbon necessary for forming skeletal structures (Zebral et al., 2019). Carbonic anhydrase expression under pH stress has been poorly studied in Pacific abalone larvae. This study showed that the expression of carbonic anhydrase in Pacific abalone larvae at 30 hpf was reduced in both alkaline and acidic conditions. Carbonic anhydrase expression was also decreased in blue mussels with treatment at low pHs on days 14 and 21. On day 21, the calcification rate also decreased (Sun et al., 2016). Low pHs may cause enzyme denaturation or inhibit enzyme-substrate interactions, thereby reducing enzyme activity (Sun et al., 2016). The inhibition of carbonic anhydrase activity may inhibit shell formation (Sun et al., 2016).

The pH stress is known to increase intracellular ROS, which causes oxidative stress (Wu et al., 2016). HSPs are crucial for mitigating pH-induced oxidative stress (Qian et al., 2012). In this study, we investigated HSP90 expression in Pacific abalone larvae cultured under various pH conditions. Although HSP90 gene expression levels fluctuated in larvae at 20 and 30 hpf, they were not significantly different. Fluctuations in HSP90 gene expression levels under pH stress with various exposure durations were also observed in vannamei shrimp (*Litopenaeus vannamei*) cultured under five different pHs (6.1, 7.1, 8.1, 9.1, and 10.1) (Qian et al., 2012). HSP expression might be upregulated as a defense mechanism (Sganga et al., 2022), while it may be downregulated owing to a reduction in the available energy resources required for HSP synthesis (Liu et al., 2012).

During the early stages of larval development of abalone (lecithotrophic), external feeding is unnecessary as they obtain their nutrition from the egg yolk (Koyama et al., 2020). Upon reaching the premetamorphic stages, larvae must find a suitable substrate and start benthic grazing at the bottom of the aquatic environment (Espinell-Velasco et al., 2021). In this study, extremely low pH (6) and high pH (10) conditions decreased the settlement rate. In 2015, Tahil & Dy (2015) suggested that reduced pH levels can cause morphological problems and delayed development, making settlement more difficult for larvae. Changes in pH can lead to a reduction in the nutritional value

of diatoms and impair the ability of larvae to recognize suitable substrates for settlement (Gómez-Reyes et al., 2023).

The pH treatment and larval age have a strong interaction effect on larval length and malformation rate. The larvae at 30 hpf experienced a longer pH exposure compared to those at 20 hpf. This can potentially result in increased damage to the larvae. Additionally, it can inhibit growth from 20 to 30 hpf in extreme acidic or alkaline pH conditions. In the correlation test, DNA damage had a strong negative correlation with hatching rate and settlement rate but a positive correlation with malformation rate in both 20 and 30 hpf larvae. This indicates that high damage to larvae DNA can lead to a high malformation rate.

## Conclusion

The study revealed that extreme pH levels affected the hatching rate, malformation rate, larval length, DNA damage, and oxygen consumption rate of early-stage abalone larvae and the settlement rate of competent larvae. Deviations in pH beyond the optimal conditions also altered carbonic anhydrase gene expression in 30 hpf larvae. However, extreme pHs did not affect the expression of the calmodulin and HSP90 genes in abalone larvae. This research contributes fundamental knowledge regarding the sensitivity of Pacific abalone larvae to extreme pH conditions.

## Competing interests

No potential conflict of interest relevant to this article was reported.

## Funding sources

This research was supported by The Korea Institute of Marine Science and Technology Promotion (KIMST), funded by the Ministry of Oceans and Fisheries (RS-2022-KS221671).

## Acknowledgements

The authors would like to thank the Korea Institute of Marine Science and Technology Promotion (KIMST) and the Ministry of Oceans and Fisheries for the funding, as well as the CEO of Haenam Hatchery for providing the fertilized eggs used in the present study.

## Availability of data and materials

Upon reasonable request, the datasets of this study can be avail-

able from the corresponding author.

## Ethics approval and consent to participate

This study conformed to the guidance of animal ethical treatment for the care and use of experimental animals.

## ORCID

Dian Yuni Pratiwi	<a href="https://orcid.org/0000-0003-2777-4199">https://orcid.org/0000-0003-2777-4199</a>
Irfan Zidni	<a href="https://orcid.org/0000-0003-4382-8513">https://orcid.org/0000-0003-4382-8513</a>
Mi-Jin Choi	<a href="https://orcid.org/0000-0003-3537-6182">https://orcid.org/0000-0003-3537-6182</a>
Young-Dae Oh	<a href="https://orcid.org/0000-0002-7408-0969">https://orcid.org/0000-0002-7408-0969</a>
Tae Min Kim	<a href="https://orcid.org/0009-0009-6336-1288">https://orcid.org/0009-0009-6336-1288</a>
Han Kyu Lim	<a href="https://orcid.org/0000-0001-8522-9901">https://orcid.org/0000-0001-8522-9901</a>

## References

- Augustyniak M, Orzechowska H, Kędzierski A, Sawczyn T, Doleżych B. DNA damage in grasshoppers' larvae – comet assay in environmental approach. *Chemosphere*. 2014;96:180-7.
- Braga AC, Pereira V, Marçal R, Marques A, Guilherme S, Costa PR, et al. DNA damage and oxidative stress responses of mussels *Mytilus galloprovincialis* to paralytic shellfish toxins under warming and acidification conditions: elucidation on the organ-specificity. *Aquat Toxicol*. 2020;228:105619.
- Caldeira K, Wickett ME. Anthropogenic carbon and ocean pH. *Nature*. 2003;425:365.
- Choi M-J, Kim YR, Park NG, Kim C-H, Oh YD, Lim HK, et al. Characterization of a C-type lectin domain-containing protein with antibacterial activity from Pacific abalone (*Haliotis discus hannai*). *Int J Mol Sci*. 2022;23(2):698.
- Espinell-Velasco N, Lamare M, Kluibenschedl A, Moss G, Cummings V. Ocean acidification induces carry-over effects on the larval settlement of the New Zealand abalone, *Haliotis iris*. In: Woodson CB, editor. *ICES J Mar Sci*. 2021. p. 340-8.
- FAO. Fishery and Aquaculture Statistics-Global Fish Trade Statistics 1976–2020. FishStaJ: Software for fishery and aquaculture statistical time series [Internet]. FAO. 2022 [cited 2024 Jul 26]. <https://www.fao.org/fishery/en/statistics/software/fishstatj>
- Ghazy MME. Effects of pH on survival, growth and reproduction rates of the crustacean. *Aust J Basic Appl Sci*. 2011;5:1-10.
- Gómez-Reyes R, Galindo-Sánchez CE, Lafarga-De La Cruz F,

- Hernández-Ayón JM, Valenzuela-Wood E, López-Galindo L. Individual pattern response to CO<sub>2</sub>-induced acidification stress in *Haliotis rufescens* suggests stage-specific acclimatization during its early life history. Sustainability. 2023;15:14010.
- Harris JO, Maguire GB, Edward SJ, Hindrum SM. Effect of pH on growth rate, oxygen consumption rate, and histopathology of gill and kidney tissue for juvenile greenlip Abalone, *Haliotis laevis* donovan and blacklip abalone, *Haliotis rubra* leach. J Shellfish Res. 1999;18:611-9.
- Hinga KR. Effects of pH on coastal marine phytoplankton. Mar Ecol Prog Ser. 2002;238:281-300.
- Huo Z, Rbbani MG, Cui H, Xu L, Yan X, Fang L, et al. Larval development, juvenile survival, and burrowing rate of geoduck clams (*Panopea japonica*) under different pH conditions. Aquacult Int. 2019;27:1331-42.
- Jiang W, Wang X, Rastrick SPS, Wang J, Zhang Y, Strand Ø, et al. Effects of elevated pCO<sub>2</sub> on the physiological energetics of Pacific oyster, *Crassostrea gigas*. ICES J Mar Sci. 2021;78:2579-90.
- Kapsenberg L, Miglioli A, Bitter MC, Tambutté E, Dumollard R, Gattuso JP. Ocean pH fluctuations affect mussel larvae at key developmental transitions. Proc R Soc B Biol Sci. 2018;285:20182381.
- Kim MJ, Kim JA, Lee DW, Park YS, Kim JH, Choi CY. Oxidative stress and apoptosis in disk abalone (*Haliotis discus hannai*) caused by water temperature and pH changes. Antioxidants. 2023;12:1003.
- Kimura R, Takami H, Ono T, Onitsuka T, Nojiri Y. Effects of elevated pCO<sub>2</sub> on the early development of the commercially important gastropod, Ezo abalone *Haliotis discus hannai*. Fish Oceanogr. 2011;20:357-66.
- Korean statistical information service (KOSIS). Domestic aquaculture production [Internet]. KOSIS. 2022 [cited 2024 Jul 29]. <http://kosis.kr/search/search.do>
- Koyama M, Furukawa F, Koga Y, Funayama S, Furukawa S, Baba O, et al. Gluconeogenesis and glycogen metabolism during development of pacific abalone, *Haliotis discus hannai*. Am J Physiol Regul Integr Comp Physiol. 2020;318:R619-33.
- Lee HB, Jang HS, Oh YD, Lee YH, Lim HK. Analysis of the physiological responses of pacific abalone (*Haliotis discus hannai*) to various stressors to identify a suitable stress indicator. J World Aquacult Soc. 2023;54:1407-26.
- Li J, Jiang Z, Zhang J, Qiu JW, Du M, Bian D, et al. Detrimental effects of reduced seawater pH on the early development of the Pacific abalone. Mar Pollut Bull. 2013;74:320-4.
- Li L, Li S, Dong Y, Yang P, Wang R. Pilot study on the deep treatment of sulfuric-acid-titanium-dioxide wastewater using an ultrafiltration/reverse osmosis process. Processes. 2023;11:1626.
- Liu W, Huang X, Lin J, He M. Seawater acidification and elevated temperature affect gene expression patterns of the pearl oyster *Pinctada fucata*. PLOS ONE. 2012;7:e33679.
- Lorenzo-Felipe Á, Shin HS, León-Bernabeu S, Pérez-García C, Zamorano MJ, Pérez-Sánchez J, et al. The effect of the deformity genetic background of the breeders on the spawning quality of gilthead seabream (*Sparus aurata* L.). Front Mar Sci. 2021;8:656901.
- Mangan S, Urbina MA, Findlay HS, Wilson RW, Lewis C. Fluctuating seawater pH/pCO<sub>2</sub> regimes are more energetically expensive than static pH/pCO<sub>2</sub> levels in the mussel *Mytilus edulis*. Proc R Soc B Biol Sci. 2017;284:20171642.
- Martel SI, Fernández C, Lagos NA, Labra FA, Duarte C, Vivanco JF, et al. Acidification and high-temperature impacts on energetics and shell production of the edible clam *Ameghinomya antiqua*. Front Mar Sci. 2022;9:972135.
- Mzozo ZB, Hugo S, Vine NG. The use of chemical and biological settlement cues in enhancing the larval settlement of abalone (*Haliotis midae*): implications for hatcheries and ocean ranching. J World Aquacult Soc. 2023;54:1702-17.
- Nagy B, Csorbai B, Várkonyi L, Staszny Á, Molnár J, Láng ZL, et al. Comparative study on the gamete quality, artificial propagation and larval development of common goldfish, shubunkin, black moor, and oranda variants of goldfish (*Carassius auratus*). Aquaculture. 2024;582:740502.
- Ono T, Muraoka D, Hayashi M, Yorifuji M, Dazai A, Omoto S, et al. Short-term variation in pH in seawaters around coastal areas of Japan: characteristics and forcings. Biogeosciences. 2024;21:177-99.
- Orr JC, Fabry VJ, Aumont O, Bopp L, Doney SC, Feely RA, et al. Anthropogenic ocean acidification over the twenty-first century and its impact on calcifying organisms. Nature. 2005;437:681-6.
- Praveen Kumar MK, Shyama SK, Sonaye BS, Naik UR, Kadam SB, Bipin PD, et al. Evaluation of  $\gamma$ -radiation-induced DNA damage in two species of bivalves and their relative sensitivity using comet assay. Aquat Toxicol. 2014;150:1-8.

- Qian Z, Liu X, Wang L, Wang X, Li Y, Xiang J, et al. Gene expression profiles of four heat shock proteins in response to different acute stresses in shrimp, *Litopenaeus vannamei*. Comp Biochem Physiol C Toxicol Pharmacol. 2012;156:211-20.
- Saad M, Shaleh FR, Rahayu AP, Fanni NA. Effect of different pH on embryogenesis and hatching rate of srikandi strain tilapia eggs (*Oreochromis aureus* × *Oreochromis niloticus*) in incubator. Indones J Limnol. 2023;3:86-94.
- Schwaner C, Barbosa M, Schwemmer TG, Pales Espinosa E, Allam B. Increased food resources help eastern oyster mitigate the negative impacts of coastal acidification. Animals. 2023; 13:1161.
- Sganga DE, Dahlke FT, Sørensen SR, Butts IAE, Tomkiewicz J, Mazurais D, et al. CO<sub>2</sub> induced seawater acidification impacts survival and development of European eel embryos. PLOS ONE. 2022;17:e0267228.
- Sharker MR, Kim SC, Hossen S, Sumi KR, Choi SK, Choi KS, et al. Carbonic anhydrase in Pacific Abalone *Haliotis discus hannai*: characterization, expression, and role in biomineralization. Front Mol Biosci. 2021;8:655115.
- Sun T, Tang X, Zhou B, Wang Y. Comparative studies on the effects of seawater acidification caused by CO<sub>2</sub> and HCl enrichment on physiological changes in *Mytilus edulis*. Chemosphere. 2016;144:2368-76.
- Tahil AS, Dy DT. Effects of reduced pH on larval settlement and survival of the donkey's ear abalone, *Haliotis asinina* (Linnaeus 1758). Philipp J Sci. 2015;144:21-9.
- Tahil AS, Dy DT. Effects of reduced pH on the early larval development of hatchery-reared donkey's ear abalone, *Haliotis asinina* (Linnaeus 1758). Aquaculture. 2016;459:137-42.
- Van Colen C, Debusschere E, Braeckman U, Van Gansbeke D, Vincx M. The early life history of the clam *Macoma balthica* in a high CO<sub>2</sub> world. PLOS ONE. 2012;7:e44655.
- Wessel N, Martin S, Badou A, Dubois P, Huchette S, Julia V, et al. Effect of CO<sub>2</sub>-induced ocean acidification on the early development and shell mineralization of the European abalone (*Haliotis tuberculata*). J Exp Mar Biol Ecol. 2018;508:52-63.
- Wu F, Lu W, Shang Y, Kong H, Li L, Sui Y, et al. Combined effects of seawater acidification and high temperature on hemocyte parameters in the thick shell mussel *Mytilus coruscus*. Fish Shellfish Immunol. 2016;56:554-62.
- Xin X, Liu C, Liu Z, Zhang Y, Gao Y, Zhu T, et al. Calmodulin regulates the calcium homeostasis in mantle of *Crassostrea gigas* under ocean acidification. Front Mar Sci. 2022;9:1050022.
- Zebral YD, da Silva Fonseca J, Marques JA, Bianchini A. Carbonic anhydrase as a biomarker of global and local impacts: insights from calcifying animals. Int J Mol Sci. 2019;20:3092.